(Received 13 June 2024, Accepted 20 August 2024, Scheduled 11 September 2024)

SRA-DGS-NL Based Decoupling Scheme for MIMO Antenna

Revati C. Godi[1, 2, *] and Rajendra R. Patil[2]

[1] *Department of E&CE, Sharnbasva University, Kalaburagi, India*
[2] *Department of E&CE, GSSS IET for Women, Mysuru*
Affiliated to Visvesvaraya Technological University, Belagavi, India

ABSTRACT: In this paper, a novel decoupling strategy for a MIMO antenna is proposed. This MIMO antenna system consists of two symmetric inverted L shaped antenna elements. To improve the isolation between radiating antenna elements, split ring arrays, neutralisation line, and ground slots are employed. The MIMO antenna operates at 6.27 GHz. Neautralization line aids in cancelling the coupling by introducing reverse coupling. Ground slots introduce band-stop characteristic to nullify the coupling effect, and split ring array blocks the electromagnetic coupling reaching the other antenna element. The isolation parameters $|S_{12}|$ and $|S_{21}|$ obtained are less than -21 dB. The diversity parameters envelope correlation coefficient and diversity gain are investigated. Envelope correlation coefficient is within acceptable limit. These diversity parameters indicate that good diversity performance is achieved by the proposed MIMO antenna. Measured results are in good agreement with simulated ones. The suggested antenna is appropriate for many wireless applications, including IEEE 802.11 and 802.16 standards, as we deal with the sensitive environment.

1. INTRODUCTION

Many modern telecommunications standards have embraced multiple antenna technology, multiple-input multiple-output (MIMO), particularly in the consumer area, because it provides significant advantages over equivalent systems that use single antenna transceivers, single-input single-output (SISO). The signalling degrees of freedom brought about by many antennas at the sender and receiver were absent from SISO systems. This refers to the spatial degree of freedom. It can be used for "diversity," "multiplexing," or a combination of the two. When the same signal is generated in numerous copies, the signal-to-noise ratio increases, increasing the chance of data delivery unaffected by fading. MIMO technology enhances radio frequency (RF) network capacity, which reduces congestion and enhances connection reliability. Wi-Fi networks and cellular 3G/4G LTE are two prominent examples of how MIMO has become more prevalent in RF/Microwave communication technologies over the past few decades. It is difficult to achieve an ideal isolation in a small package, although they can greatly enhance the channel capacity.

Numerous methods for improving antenna element isolation to decrease the coupling impact are available in the literature.

To increase isolation, MIMO antenna design incorporates polarisation diversity technique. An excellent isolation performance is achieved by placing the two feed points orthogonally, which guarantees that each planar inverted F-shape antenna (PIFA)'s dominant polarisation is opposite to the other [1]. To increase isolation at the lower band edge, a rectangular slit was added from the bottom left of the ground plane. The slit on the ground plane causes a noticeable decrease in surface current density [2]. With loaded inverted L-monopole antenna elements using split-ring resonators (SRRs), an improved level of isolation is found by presenting a MIMO architecture in which SRRs inhibit the overall inter-element interaction [3].

Two similar monopole antenna (MA) elements are positioned on one side of the substrate. Assigning the opposite side of the substrate to the ground plane with the flag-shaped stub lowering mutual coupling and promoting the isolation between antenna elements. It is demonstrated that the new coupling path generated by the flag-shaped stub cancels out the originally established coupling between the MAs [4]. Partially extended ground (PEG) arm and ground stub lead to lower coupling between two ports and a restriction on the current to link [5].

In order to control the mutual coupling between radiators, the MIMO antenna is connected to each partial ground and employs a T-shaped isolator to restrict the coupling effects [6]. The antenna is made up of two radiating patches with symmetric L-shaped slots and folded microstrip lines. An isolation line connects the two patches to lessen the coupling effect between ports. CSSRs are used to regulate resonance frequencies and improve isolation. To strengthen the isolation between the ports and neutralise mutual coupling, an isolation line is connected between the two rectangular radiation elements [7]. In order to reduce the mutual coupling between the radiating patches, a neutralisation line is used. The current is flowing in the opposite direction on the rectangular strip and at the centre ground plane. This results in the field being cancelled, which improves the isolation between the two radiating elements [8]. Its ground plate includes four inverted L-shaped grooves etched into it to reduce the mutual interaction between adjacent antenna elements [9].

Electromagnetic band gaps (EBGs) are structures that have been utilised to reduce mutual contact between antenna ele-

* Corresponding author: Revati C. Godi (revatigodi@gmail.com).

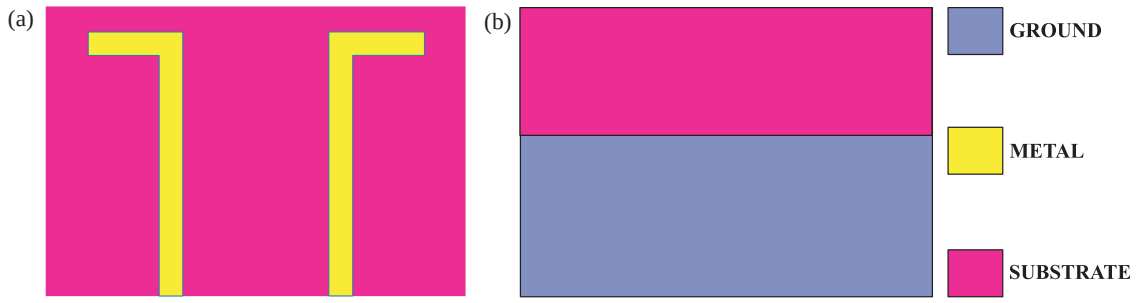

FIGURE 1. Schematic of (a) top view and (b) bottom view of a designed two element MIMO antenna without SRA-DGS-NL.

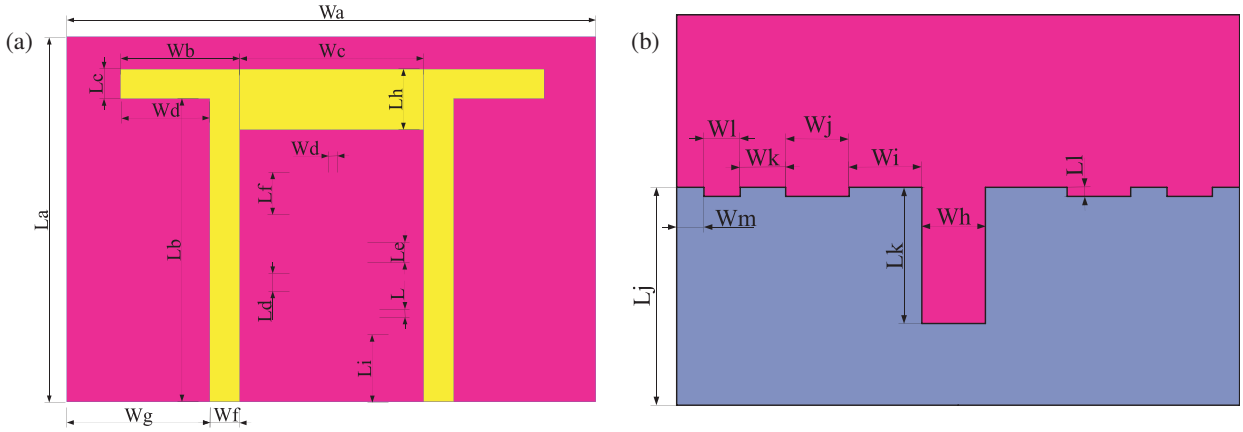

FIGURE 2. Schematic of (a) top view and (b) bottom view of a designed two element MIMO antenna with SRA-DGS-NL.

ments. The EBG configuration's resonance indicates that the EBG edge impedance is very strong close to the resonant frequency, which causes waves striking the EBG structure to be reflected in phase [10]. In order to provide stronger isolation between the elements, L-shaped meta-rim extended ground stubs provide an additional longer electrical channel for surface current between the two ports [11].

The MIMO configuration uses three sets of hexagon-shaped split ring resonators (HSRRs) to provide decoupling. A frequently employed synthetic magnetic material is split ring resonator. Its band-stop filter properties help decrease coupling currents in addition to efficiently countering the free-space coupling between the MIMO sections [12]. A switchable band-stop filter is employed as a decoupling mechanism to develop a small reconfigurable MIMO antenna [13]. The issue of mutual separation between adjacent radiating elements has been enhanced with the inclusion of a vertical decoupling strip to the rear of the two-port diversity MIMO antenna [14].

A unique complementary modified Minkowski fractal (CMMF) is suggested to be used in a smaller U-formed ultra-wideband (UWB) MIMO antenna for isolation enhancement. A specifically modified Minkowski fractal-shaped slot was added to the ground plane to boost isolation. It is noted that there is enough current coupled close to the CMMF. As a result, CMMF decreased the coupled current density close to the UWB-MIMO antenna's second U-shaped monopole element [15]. To enhance the isolation in the sub-6 GHz band, a Dual Negative unit cell isolator, inspired by metamaterials, is placed precisely across the side of the tightly spaced antenna elements. The redesigned W-shaped antenna elements contain an isolator, which is a 2×1 array of metamaterial unit cells. The metamaterial unit cell array's effective enhancement in isolation level is confirmed by the surface current suppression [16]. Compared to side-by-side arrangement, the orthogonal orientation improves the isolation between antenna parts [17].

In this paper, the novelty in decoupling structure is introduced which includes neutralization line (NL), defective ground structure (DGS), and split ring array (SRA) in order to lower the coupling effect.

2. MIMO ANTENNA DESIGN AND FABRICATION

In this section, a detailed antenna design and its schematic is illustrated. Further, figures of fabricated prototype of MIMO antenna (i) without SRA-DGS-NL (ii) with SRA-DGS-NL are also presented.

2.1. Fabrication of Designed Two Element MIMO Antenna

In this section, figures of a schematic and fabricated two element MIMO antenna have been provided.

Figures 1 and 2 show the schematic of top and bottom views of a MIMO antenna without and with SRA-DGS-NL, respec-

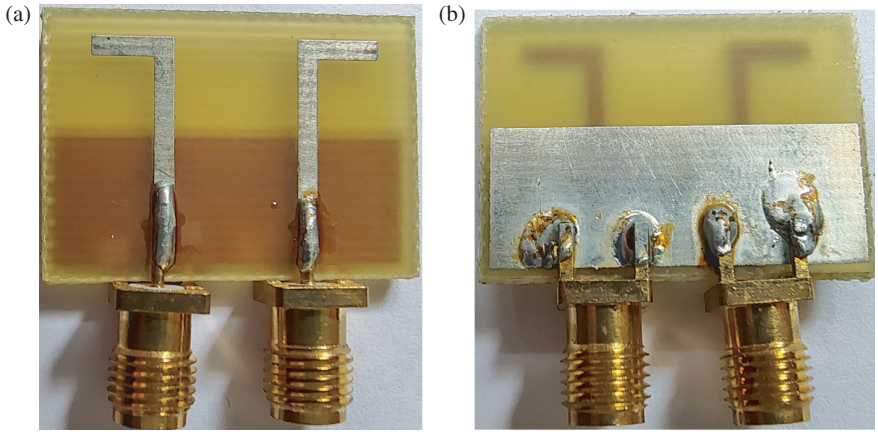

FIGURE 3. Photographs of (a) top view and (b) bottom view of a designed two element MIMO antenna without SRA-DGS-NL.

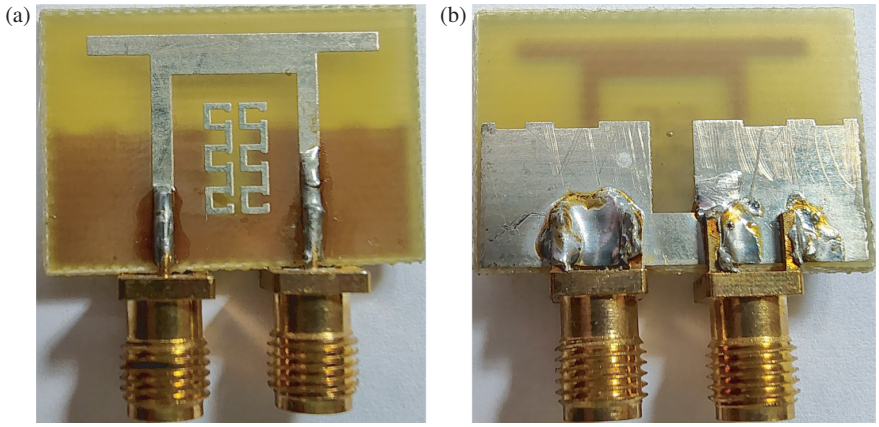

FIGURE 4. Photographs (a) top view and (b) bottom view of a designed two element MIMO antenna with SRA-DGS-NL.

tively. Further, Figs. 3 and 4 show photographs of the corresponding fabricated prototypes. The design concept calls for the placement of identical inverted L-shaped antenna elements fed by microstrip feeding on top of the dielectric substrate. Slots are etched into the ground plane to improve impedance matching and isolation between the antenna elements. The substrate used is epoxy FR4, which has a thickness of 1.6 mm and a dielectric constant of 4.4. The antenna resonates at 6.27 GHz and takes up a very small space $(18 \times 26\,\text{mm}^2)$. Spit ring array is included between the antenna elements to reduce the coupling effect.

Table 1 gives the detailed dimension of a two-element MIMO antenna considered in this study.

3. RESULTS AND DISCUSSION

The proposed antenna has been simulated using commercially available ANSYS HFSS simulation software, and various parameters such as S-parameters, gain and radiation patterns are investigated and extracted for MIMO antenna without and with SRA-DGS-NL.

TABLE 1. Dimensions of the two element MIMO antenna.

Parameters	Dimesnions (mm)	Parameters	Dimesnions (mm)
Wa	26.0	La	18.0
Wb	6.0	Lb	15.0
Wc	9.0	Lc	1.5
Wd	4.5	Ld	1.0
We	0.5	Le	1.0
Wf	1.5	Lf	2.0
Wg	7.0	Lg	0.5
Wh	3.0	Lh	3.0
Wi	3.5	Li	3.5
Wj	3.0	Lj	10.0
Wk	2.0	Lk	6.5
Wl	2.0	Ll	0.5
Wm	1.0		

3.1. Simulated and Measured S-Parameters

Figure 5 shows the simulated results of return loss $|S_{11}|$ and mutual coupling coefficient $|S_{12}|$ for both the cases, i.e., without

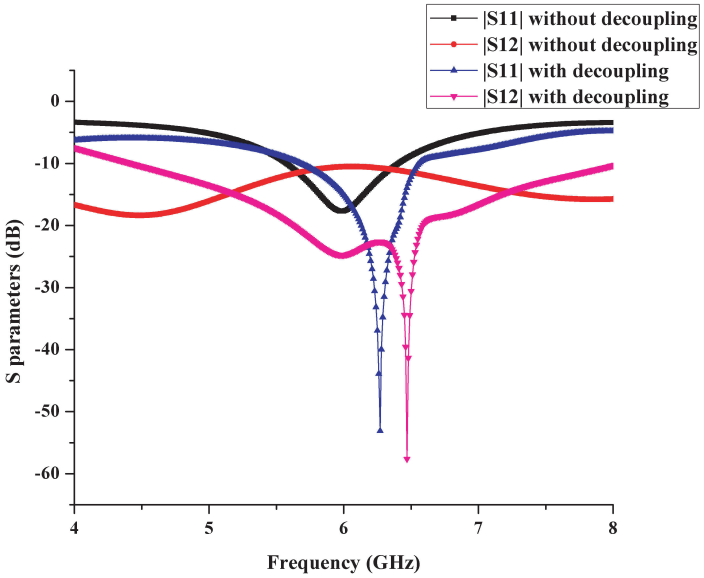

FIGURE 5. Simulated $|S_{11}|$ and $|S_{12}|$ of a MIMO antenna without and with decoupling structure.

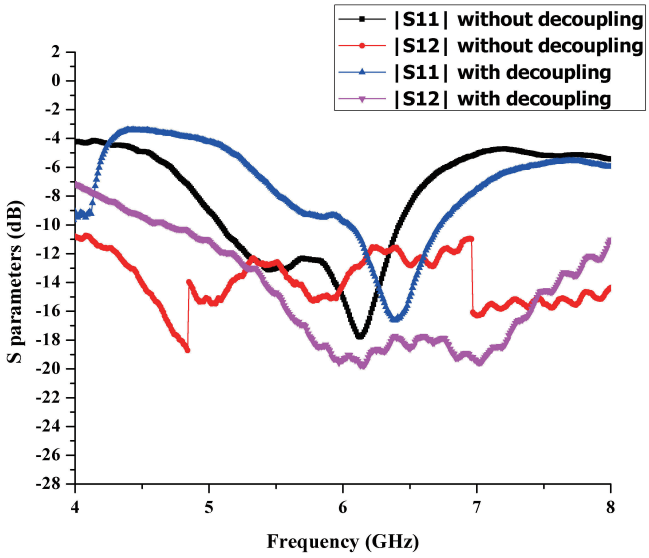

FIGURE 6. Measured (a) $|S_{11}|$ and $|S_{12}|$ of a MIMO antenna without and with decoupling structure.

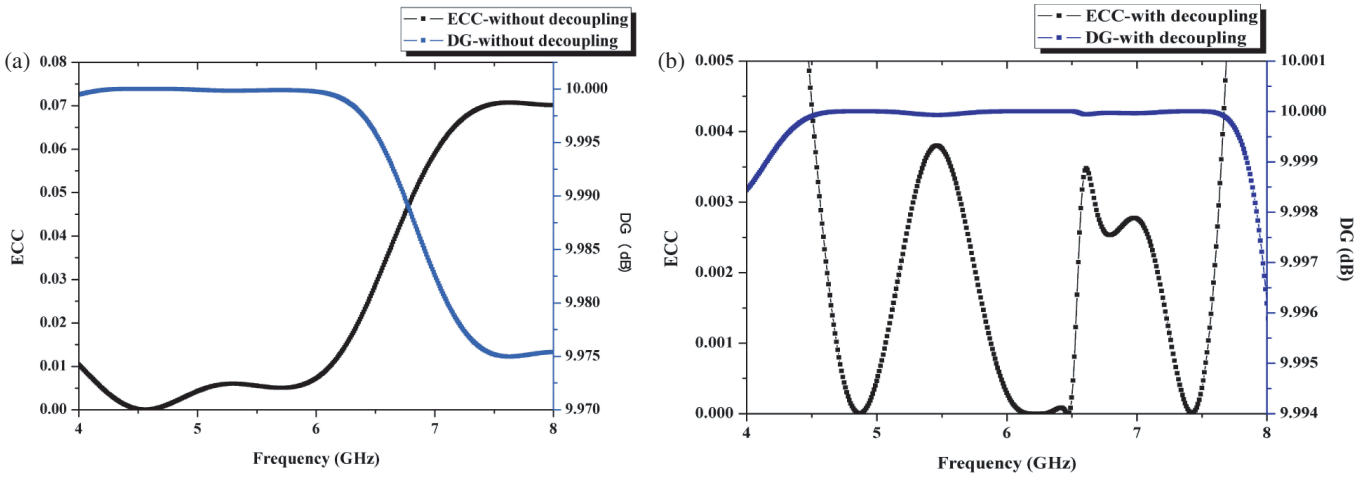

FIGURE 7. Simulated DG and ECC. (a) Without SRA-DGS-NL. (b) With SRA-DGS-NL.

and with SRA-DGS-NL. From the figure it is seen that, in the case of without SRA-DGS-NL, antenna resonates at 5.99 GHz with return loss $|S_{11}|$ being -17.71 dB, mutual coupling coefficient $|S_{12}|$ below -10.51 dB, and gain of the antenna being 1.77 dBi. With SRA-DGS-NL, antenna resonates at 6.27 GHz, with $|S_{11}|$ being -53.10 dB, $|S_{12}|$ being -21 dB, and gain obtained being 2 dBi. A slight shift in the resonant frequency as compared to that without SRA-DGS-NL decoupling structure is seen and is due to insertion of split ring array which adds reactive loading effect to the structure. The reactive loading effect causes changes to the reactive elements value, i.e., inductance and capacitance variations due to which drift in the resonant frequency is observed. $|S_{22}|$ and $|S_{21}|$ parameters are the same as that of $|S_{11}|$ and $|S_{12}|$, respectively as the two antenna elements are identical. The inference made on the results is that isolation enhancement around 10.5 dB is obtained by including SRA-DGS-NL decoupling structure.

Experimental investigation is carried out with the help of a vector network analyzer. Fig. 6 represents the measured results for the above mentioned s-parameters. Analysis on the results depicts that measured and simulated results are in good agreement.

3.2. Diversity Performance

In applications involving diversity and MIMO, the correlation among signals obtained by the corresponding antennas at the side of a wireless link is a critical aspect in determining the effectiveness of the system. The envelope correlation coefficient is frequently used to assess a multi-antenna system's diversity capabilities.

In general, the far-field radiation pattern [18, 19] or the scattering parameters from the antenna system [20] can be used to calculate the envelope correlation coefficient of an antenna ar-

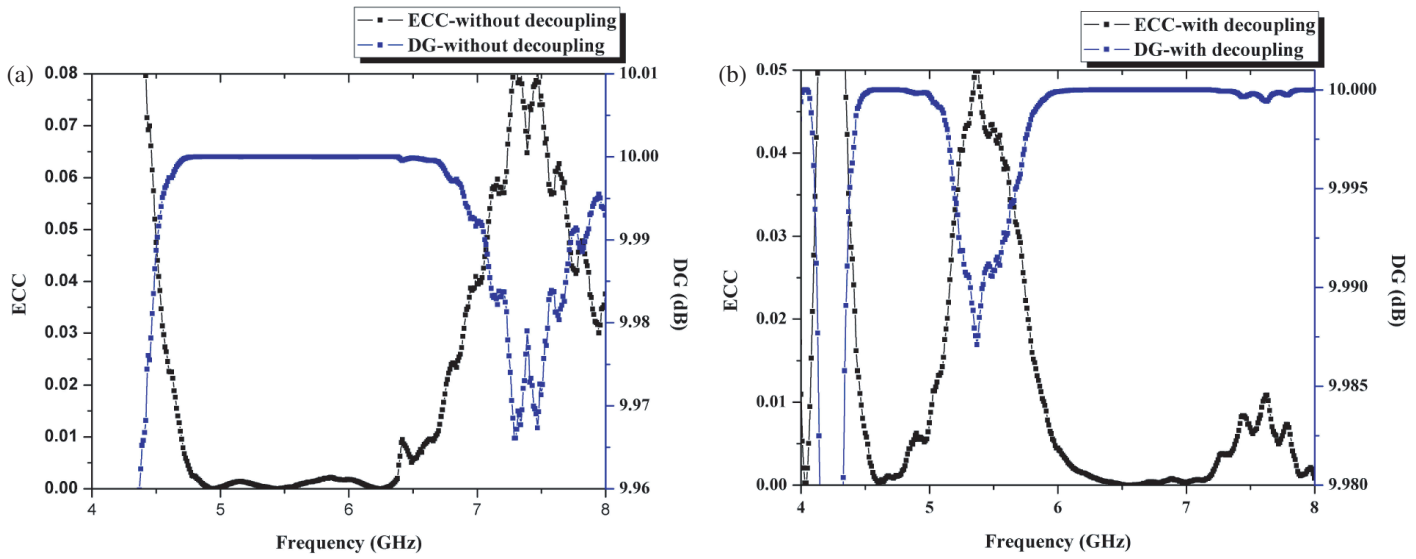

FIGURE 8. Measured DG and ECC. (a) Without SRA-DGS-NL. (b) With SRA-DGS-NL.

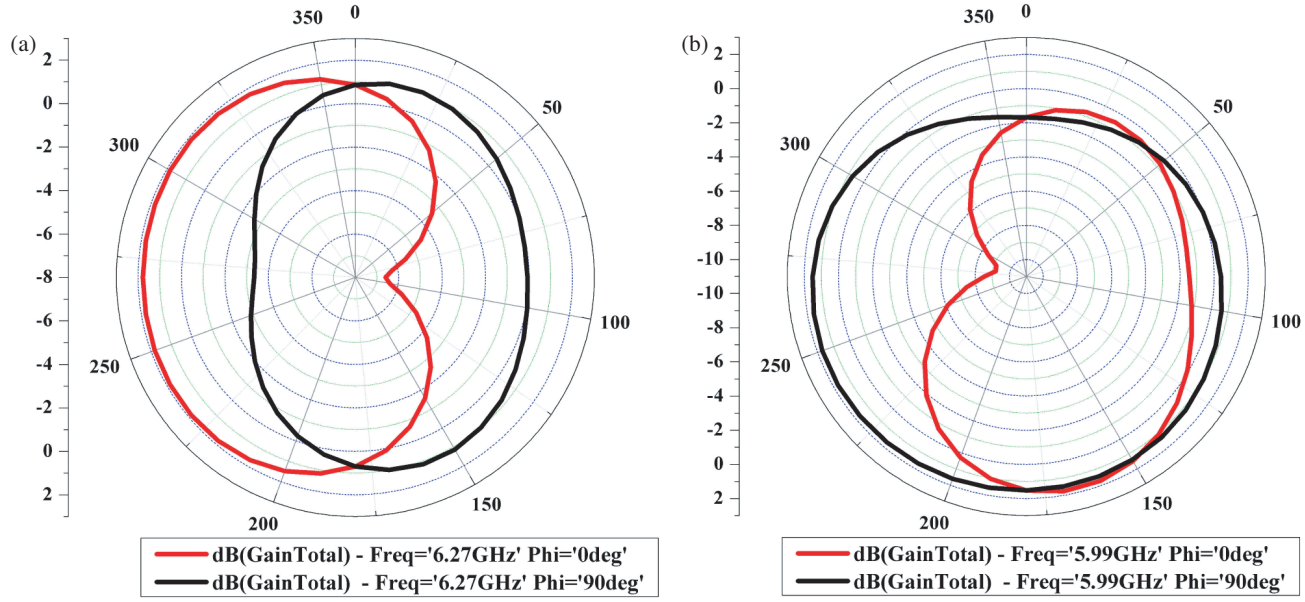

FIGURE 9. Simulated radiation pattern. (a) Without SRA-DGS-NL. (b) With SRA-DGS-NL.

ray. According to [20], the following equation may be used to calculate the envelope correlation coefficient ρ_e (See Eq. (1) of a two antenna system):

$$\rho_e = \frac{|S_{11}^* S_{12} + S_{21}^* S_{22}|^2}{(1 - |S_{11}|^2 - |S_{21}|^2)(1 - |S_{22}|^2 - |S_{12}|^2)} \quad (1)$$

Envelope correlation coefficient $\rho_e < 0.5$ is the acceptable limit for good diversity performance.

Another diversity parameter is diversity gain (DG). It defines how well a signal is transmitted with the minimum loss during transmission. It is given by the following expression (see Eq. (2)) [20]

$$DG = 10\sqrt{1 - |\rho_e|^2} \quad (2)$$

Figures 7(a) and 7(b) show the simulated DG and ECC for the MIMO antenna without and with SRA-DGS-NL, and Figs. 8(a) and 8(b) show the measured DG and ECC for the MIMO antenna without and with SRA-DGS-NL. From the figure it is observed that ECC is much reduced when the decoupling structure is included and found to be less than 0.0027, and diversity gain (DG) is nearly 10 dB. Therefore, the proposed work suggests that diversity parameters are excellent, and antenna elements are well isolated from one another.

Radiation patterns at $\phi = 0°$ and $\phi = 90°$ for the two element MIMO antenna without and with SRA-DGS-NL are as shown in Figs. 9(a) and 9(b), respectively. From the figures it is observed that stable and omnidirectional radiation patterns are obtained. Figs. 10(a) and 10(b) depict the measured radiation

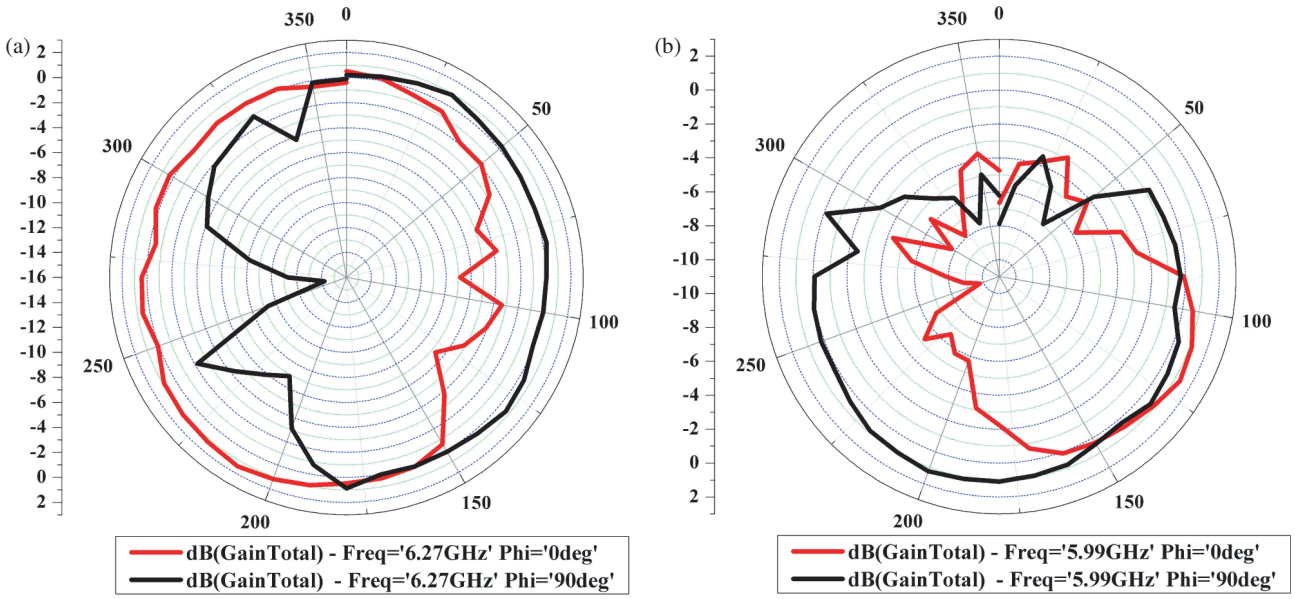

FIGURE 10. Measured radiation pattern. (a) Without SRA-DGS-NL. (b) With SRA-DGS-NL.

TABLE 2. Performance evaluation of two element MIMO antenna.

Antenna Configuration		Resonant frequency (GHz)	$\|S11\|$ (dB)	$\|S12\|$ (dB)	$\|S22\|$ (dB)	$\|S21\|$ (dB)	ECC	DG (dB)
Without SRA-DGS-NL	Simulated	5.99	−17.71	−10.51	−17.71	−10.51	0.023	9.99732
	Measured	6.13	−17.80	−11.53	−17.80	−11.53	0.01	9.99955
With SRA-DGS-NL	Simulated	6.27	−53.10	−21	−53.10	−21	0.0027	9.999963
	Measured	6.39	−16.64	−17.73	−16.64	−17.73	0.0033	9.999943

TABLE 3. Comparison of parameters considered in the present study with the published work.

Ref.	Antenna size (mm × mm)	Resonant Frequency (GHz)	Isolation (dB)	ECC	DG
[12]	45 × 40	5.08–6.30	< -25	< 0.1	-
[21]	20 × 34	2.11–4.19 4.98–6.81	< -21	< 0.004	> 9.97
[22]	100 × 60	2.4, 5.2 and 5.8	< -18, < -38, and < -34	< 0.04	-
[23]	18.5 × 56	2.5, 3.7, 4.3 and 5.5	< -20	<0.05	> 9.98
Present study	18 × 26	5.68–6.56	< -21	< 0.0027	> 9.99

patterns at $\phi = 0°$ and $\phi = 90°$ degree which have a good agreement with the simulated results.

Table 2 shows the performance evaluation of Two Element MIMO Antenna, from the data it can be infer that mutual coupling with SRA-DGS-NL is reduced by about 10.5 dB compared to mutual coupling without SRA-DGS-NL. The measured and simulated readings correlate well with each other. The influence of SMA connector soldering, substrate losses, and measurement conditions are the causes of the slight variations between the measured and simulated findings.

3.3. Comparison and Implications

Table 3 summarises the performance of proposed MIMO antenna reported in this article compared to the published research. The obtained results are summarised according to the number of parameters, including isolation, frequency band, antenna size, ECC, and DG. From the data reported in Table 3, it is noted that the suggested MIMO antenna has a few standout features, including strong isolation, decreased ECC, and enhanced DG, all of which point towards good diversity performance.

4. CONCLUSIONS

This paper has described a two-port MIMO antenna that utilises an SRA-DGS-NL decoupling network. The antenna resonance and isolation achieved are 6.27 GHz and below −21 dB. The comparison made without and with SRA-DGS-NL decoupling network indicates that isolation enhancement around 10.5 dB is obtained with SRA-DGS-NL. The envelope correlation coefficient of less than 0.0027 is achieved, and diversity gain close to 10 dB is achieved. The isolation improvement is due to DGS which acts as a band-stop filter, split ring which blocks the radiations coupling to the other antenna element, and neutralization line reverses the coupling effect. The findings obtained show that the suggested antenna performs well in terms of diversity and is appropriate for a range of wireless applications, including WiLAN, WiMAX, and sub-6 GHz applications.

REFERENCES

[1] Han, M. and J. Choi, "Dual-band MIMO antenna using polarization diversity for 4G mobile handset application," *Microwave and Optical Technology Letters*, Vol. 53, No. 9, 2075–2079, 2011.

[2] Marzudi, W. N. N. W., Z. Z. Abidin, S. H. Dahlan, M. Yue, R. A. Abd-Alhameed, and M. B. Child, "A compact orthogonal wideband printed MIMO antenna for WiFi/WLAN/LTE applications," *Microwave and Optical Technology Letters*, Vol. 57, No. 7, 1733–1738, 2015.

[3] Sarkar, D. and K. V. Srivastava, "Compact four-element SRR-loaded dual-band MIMO antenna for WLAN/WiMAX/WiFi/4G-LTE and 5G applications," *Electronics Letters*, Vol. 53, No. 25, 1623–1624, 2017.

[4] Katie, M. O., M. F. Jamlos, A. S. M. Alqadami, and M. A. Jamlos, "Isolation enhancement of compact dual-wideband MIMO antenna using flag-shaped stub," *Microwave and Optical Technology Letters*, Vol. 59, No. 5, 1028–1032, 2017.

[5] Malviya, L., M. V. Kartikeyan, and R. K. Panigrahi, "Multi-standard, multi-band planar multiple input multiple output antenna with diversity effects for wireless applications," *International Journal of RF and Microwave Computer-Aided Engineering*, Vol. 29, No. 2, e21551, 2019.

[6] Malviya, L., M. V. Kartikeyan, and R. K. Panigrahi, "Offset planar MIMO antenna for omnidirectional radiation patterns," *International Journal of RF and Microwave Computer-Aided Engineering*, Vol. 28, No. 6, e21274, 2018.

[7] Asadpor, L. and M. Rezvani, "Multiband microstrip mimo antenna with CSRR loaded for GSM and LTE applications," *Microwave and Optical Technology Letters*, Vol. 60, No. 12, 3076–3080, 2018.

[8] Tiwari, R. N., P. Singh, and B. K. Kanaujia, "A compact UWB MIMO antenna with neutralization line for WLAN/ISM/mobile applications," *International Journal of RF and Microwave Computer-Aided Engineering*, Vol. 29, No. 11, e21907, 2019.

[9] Xu, Z., Q. Zhang, and L. Guo, "A printed multiband MIMO antenna with decoupling element," *International Journal of Microwave and Wireless Technologies*, Vol. 11, No. 4, 413–419, 2019.

[10] Beigi, P., M. Rezvani, Y. Zehforoosh, J. Nourinia, and B. Heydarpanah, "A tiny EBG-based structure multiband MIMO antenna with high isolation for LTE/WLAN and C/X bands applications," *International Journal of RF and Microwave Computer-Aided Engineering*, Vol. 30, No. 3, e22104, 2020.

[11] Duan, J., K. Xu, X. Li, S. Chen, P. Zhao, and G. Wang, "Dual-band and enhanced-isolation MIMO antenna with L-shaped meta-rim extended ground stubs for 5G mobile handsets," *International Journal of RF and Microwave Computer-Aided Engineering*, Vol. 29, No. 8, e21776, 2019.

[12] Singh, H. V., D. V. S. Prasad, S. Tripathi, and A. Mohan, "Closely-coupled wideband MIMO antenna with isolation improvement using decoupling circuit and hexagonal split-ring resonators," *Microwave and Optical Technology Letters*, Vol. 63, No. 10, 2614–2620, 2021.

[13] Islam, H., S. Das, T. Ali, T. Bose, S. Kumari, O. Prakash, and P. Kumar, "Bandstop filter decoupling technique for miniaturized reconfigurable MIMO antenna," *IEEE Access*, Vol. 10, 19 060–19 071, 2022.

[14] Bhattacharya, A., B. Roy, S. K. Chowdhury, and A. K. Bhattacharjee, "An isolation enhanced, printed, low-profile UWB-MIMO antenna with unique dual band-notching features for WLAN and WiMAX," *IETE Journal of Research*, Vol. 68, No. 1, 496–503, 2022.

[15] Gurjar, R., D. K. Upadyay, B. Kanaujia, and A. Kumar, "A compact U-shaped UWB-MIMO antenna with novel complementary modified minkowski fractal for isolation enhancement," *Progress In Electromagnetics Research C*, Vol. 107, 81–96, 2021.

[16] Sharma, R., R. Khanna, and Geetanjali, "Compact sub-6 GHz and mmwave 5G wideband 2 × 1 MIMO antenna with high isolation using parasitically placed double negative (DNG) isolator," *Wireless Personal Communications*, Vol. 122, No. 3, 2839–2857, 2022.

[17] Sabek, A. R., W. A. E. Ali, and A. A. Ibrahim, "Minimally coupled two-element MIMO antenna with dual band (28/38 GHz) for 5G wireless communications," *Journal of Infrared, Millimeter, and Terahertz Waves*, Vol. 43, No. 3, 335–348, 2022.

[18] Vaughan, R. G. and J. B. Andersen, "Antenna diversity in mobile communications," *IEEE Transactions on Vehicular Technology*, Vol. 36, No. 4, 149–172, 1987.

[19] Bhatti, R. A., J.-H. Choi, and S.-O. Park, "Quad-band MIMO antenna array for portable wireless communications terminals," *IEEE Antennas and Wireless Propagation Letters*, Vol. 8, 129–132, 2009.

[20] Blanch, S., J. Romeu, and I. Corbella, "Exact representation of antenna system diversity performance from input parameter description," *Electronics Letters*, Vol. 39, No. 9, 705–707, 2003.

[21] Tiwari, R. N., P. Singh, B. K. Kanaujia, S. Kumar, and S. K. Gupta, "A low profile dual band MIMO antenna for LTE/Bluetooth/Wi-Fi/WLAN applications," *Journal of Electromagnetic Waves and Applications*, Vol. 34, No. 9, 1239–1253, 2020.

[22] Roy, S. and U. Chakraborty, "Mutual coupling reduction in a multi-band MIMO antenna using meta-inspired decoupling network," *Wireless Personal Communications*, Vol. 114, No. 4, 3231–3246, 2020.

[23] Rasool, M., I. Rashid, A. Rauf, A. Masood, F. A. Bhatti, and B. Ijaz, "A multi-slotted 2-element quadband MIMO antenna for 4G and 5G applications," *Journal of Electromagnetic Waves and Applications*, Vol. 35, No. 15, 2062–2077, 2021.